Clinical & Translational Immunology

Australian and New Zealand Society for Immunology Inc.

Clinical & Translational Immunology 2020; e1140. doi: 10.1002/cti2.1140
www.wileyonlinelibrary.com/journal/cti

ORIGINAL ARTICLE

Synovial fluid CD69$^+$CD8$^+$ T cells with tissue-resident phenotype mediate perforin-dependent citrullination in rheumatoid arthritis

Jae Hyung Jung[1], Jung Sun Lee[2], Yong-Gil Kim[3], Chang-Keun Lee[3], Bin Yoo[3], Eui-Cheol Shin[1] & Seokchan Hong[3]

[1]Graduate School of Medical Science and Engineering, Korea Advanced Institute of Science and Technology (KAIST), Daejeon, 34141, Korea
[2]Division of Rheumatology, Department of Internal Medicine, Seoul Veterans Hospital, Seoul, Korea
[3]Division of Rheumatology, Department of Internal Medicine, Asan Medical Center, University of Ulsan College of Medicine, Seoul, Korea

Correspondence
S Hong, Division of Rheumatology, Asan Medical Center, University of Ulsan College of Medicine, 88, Olympic-ro 43-gil, Songpa-gu, Seoul 05505, Korea.
E-mail: medivineluke@gmail.com
E-C Shin, Laboratory of Immunology and Infectious Diseases, Graduate School of Medical Science and Engineering, KAIST, 291 Daehak-ro, Yuseong-gu, Daejeon 34141, Korea.
E-mail: ecshin@kaist.ac.kr

Received 29 December 2019;
Revised 13 April 2020;
Accepted 29 April 2020

doi: 10.1002/cti2.1140

Clinical & Translational Immunology
2020; **9**: e1140

Abstract

Objectives. Although the importance of tissue-resident memory T (T_{RM}) cells in organ-specific chronic inflammation has been recognised, little is known about their role in rheumatoid arthritis (RA). Here, we examined the characteristics of synovial fluid CD8$^+$ T cells that express canonical T_{RM} markers CD69 and CD103, and their role in the pathogenesis of RA. **Methods.** Synovial fluid mononuclear cells (SFMCs) were obtained from patients with RA. Flow cytometric analysis of surface markers and cytotoxic molecules of CD8$^+$ T cells was performed. TCR repertoire of CD8$^+$ T cells was analysed by TCRVβ CDR3 sequencing. Citrullination with the formation of neutrophil extracellular trap (NET) was evaluated by immunofluorescence staining. **Results.** The frequency of CD8$^+$ T cells was increased in SFMCs, and these CD8$^+$ T cells were primarily comprised of CD45RA$^-$ memory T cells expressing CD69 and/or CD103. CD69$^+$CD8$^+$ T cells exhibited T_{RM} phenotypes, including upregulation of CXCR6, CD49a and CD101, and downregulation of S1PR1 and KLF2. TCR repertoire analysis showed that these cells were an oligoclonally expanded population with increased expression of cytotoxic molecules. The treatment of neutrophils with supernatant from IL-15-stimulated CD69$^+$CD8$^+$ T cells induced perforin-mediated histone citrullination and NET formation irrespective of their CD103 expression. The frequency of perforin-expressing cells among CD69$^+$CD8$^+$ T cells in SFMCs was significantly higher in patients with anti-citrullinated protein antibody (ACPA) than in those without ACPA. **Conclusion.** CD69$^+$CD8$^+$ T cells in the SFMCs of RA patients exhibit T_{RM}-like features. These cells may participate in the pathogenesis of RA via perforin-mediated citrullination.

Keywords: rheumatoid arthritis, CD8$^+$ T cells, tissue-resident memory T cells, citrullination, ACPA

INTRODUCTION

Rheumatoid arthritis (RA) is a chronic autoimmune disease characterised by joint swelling and destruction.[1] The hallmark manifestations of RA include hyperplastic synovial tissue, immune cell infiltration and the presence of autoantibodies, such as anti-citrullinated protein antibody (ACPA).[2] Among the various types of immune cells, $CD4^+$ T cells have been the focus of many research efforts because of their capacity to produce pro-inflammatory cytokines (e.g. IFN-γ and IL-17A)[3-7] and their ability to help autoantibody-producing B-cell maturation.[8] In contrast, the role of $CD8^+$ T cells in the pathogenesis of RA remains unclear. Previous studies have reported contradicting results related to $CD8^+$ T cells in RA patients, such as the presence of anti-inflammatory IL-10-producing $CD8^+$ suppressor T cells,[9] $CD8^+$ T cells expressing pro-inflammatory IL-6 and TNF-α,[10] and resistance to regulatory T (T_{reg}) cell-mediated suppression by killing T_{reg} cells.[11]

Memory T cells provide rapid and effective protection against previously encountered antigens. However, when memory T cells pathologically accumulate and function in response to innocuous targets, such as self-antigens, these cells can contribute to the pathogenesis of autoimmune diseases. Recent studies have identified the presence of a new subset of memory $CD8^+$ T cells that reside in peripheral tissues without recirculation, tissue-resident memory T (T_{RM}) cells, which express the characteristic markers $S1P_1$ antagonist CD69[12,13] and/or adhesion protein CD103 (integrin α_E).[14,15] These cells are located in various anatomical sites, including the skin, lungs and liver,[16,17] where they provide in situ immunosurveillance and protective immunity with their ability to respond rapidly.[18,19] T_{RM} cells have been suggested to participate in the pathogenesis of autoimmune diseases.[20-23] The number of $CD103^+CD8^+$ T cells secreting IFN-γ is markedly increased in the epidermis of patients with vitiligo.[20] In addition, a recent study demonstrated that clonally expanded $CD8^+$ T cells in the synovial fluid (SF) of patients with juvenile idiopathic arthritis exhibit a feature of T_{RM} cells, suggesting that they may contribute to the disease pathology.[24]

Neutrophil extracellular trap (NET), a form of neutrophil cell death, is thought to be involved in the pathogenesis of RA by providing citrullinated autoantigens. This complex contains various intracellular proteins, including citrullinated histones, which can then influence the generation of ACPA[25] in RA patients. Furthermore, a recent study demonstrated that cytotoxic molecules released by $CD8^+$ T cells, such as perforin, can induce the formation of citrullinated proteins as well as the extracellular release of DNA.[26] Therefore, cytotoxic $CD8^+$ T cells may contribute to the pathogenesis of RA through perforin-mediated production of citrullinated histones with NET formation, and subsequent generation of ACPA.[25]

In the present study, we investigated the phenotypic, transcriptional and functional characteristics of $CD69^+CD103^+CD8^+$ and $CD69^+CD103^-CD8^+$ T cells in the SF of RA patients. We also investigated the role of $CD69^+CD8^+$ T cells in RA, especially related to formation of citrullinated histones.

RESULTS

Synovial fluid $CD8^+$ T cells from RA patients are predominantly memory cells expressing CD69 and/or CD103

First, we analysed the frequency of $CD8^+$ T cells among peripheral blood mononuclear cells (PBMCs) and synovial fluid mononuclear cells (SFMCs) from patients with RA. We also analysed their expression of CD45RA. $CD8^+$ T cells were identified based on CD3 and CD8 expression and the lack of CD14, CD19, CD56 and TCR$\gamma\delta$ expression (Supplementary figure 1). The frequency of $CD8^+$ T cells in the lymphocyte gate was higher among SFMCs from RA patients than PBMCs from RA patients or healthy controls (Figure 1a). Most of the $CD8^+$ T cells found among SFMCs were memory cells lacking CD45RA expression (Figure 1b). To evaluate tissue-residency marker expression in $CD8^+$ memory T cells, we examined the expression of CD69 and CD103 in $CD45RA^-CD8^+$ T cells. SF $CD45RA^-CD8^+$ T cells derived from RA patients were markedly enriched with $CD69^+CD103^-$ and $CD69^+CD103^+$ cells (Figure 1c). An analysis of the memory T-cell subset ($CD45RA^-$) within SF $CD8^+$ T cells showed that the proportion of effector memory T cells was higher in the $CD69^+CD103^-$ and $CD69^+CD103^+CD8^+$ T-cell subsets than in the $CD69^-CD103^-CD8^+$ T-cell subset (Figure 1d). Histopathological examination confirmed the presence of $CD69^+CD103^{+/-}CD8^+$ T cells in synovial tissues from RA patients and their absence from

synovial tissues from OA patients (Figure 1e). These findings indicate that RA patients have an increased frequency of $CD69^+CD103^{+/-}CD8^+$ T cells in their joints.

$CD69^+CD103^{+/-}CD45RA^-CD8^+$ T cells exhibit tissue-resident features

Next, we examined the phenotypes of $CD69^+CD103^{+/-}CD45RA^-CD8^+$ T cells among SFMCs from RA patients. The expression of proteins known to be upregulated in T_{RM} cells (e.g. C-X-C chemokine receptor 6 [CXCR6], CD49a and CD101) was significantly higher in $CD69^+CD103^+$ and $CD69^+CD103^-$ than in $CD69^-CD103^-CD45RA^-CD8^+$ cells (Figure 2a). The $CD103^+$ subset exhibited significantly higher expression of CXCR6, CD49a and CD101 than the $CD103^-$ subset (Figure 2a). In addition, the mRNA expression of the tissue egress protein S1PR1 and its transcription factor, KLF2, was significantly downregulated in $CD69^+CD103^+$ and $CD69^+CD103^-$ compared to $CD69^-CD103^-CD45RA^-CD8^+$ T cells (Figure 2b). Furthermore, HLA-DR and PD-1 expression was significantly higher in $CD69^+CD103^+$ and $CD69^+CD103^-$ than in $CD69^-CD103^-$ cells, with $CD69^+CD103^+CD45RA^-CD8^+$ T cells exhibiting the highest expression (Figure 2c). The expression of activation markers CD25 and CD38 was not significantly different between the $CD69^-CD103^-$ and $CD69^+CD103^{+/-}CD45RA^-CD8^+$ T-cell subsets (Supplementary figure 2). The frequency of $Ki\text{-}67^+$ cells was highest in the $CD69^+CD103^+$ T-cell subset, followed by $CD69^+CD103^-$ and $CD69^-CD103^-CD45RA^-CD8^+$ T cells (Figure 2d).

To further understand the differentiation profile of SF $CD8^+$ T cells, we investigated the expression of transcription factors associated with T-cell differentiation. The frequency of $T\text{-}bet^+$ cells was similar among the three subsets, whereas the frequency of $Eomes^+$ cells was higher among $CD69^+CD103^+$ and $CD69^+CD103^-CD45RA^-CD8^+$ T cells (Figure 2e). Collectively, $CD69^+CD103^{+/-}CD8^+$ memory T cells exhibit tissue-resident phenotypes with effector-like features.

$CD69^+CD103^{+/-}CD45RA^-CD8^+$ T-cell populations exhibit increased clonal expansion with less diversity

We also investigated whether $CD69^+CD103^{+/-}CD8^+$ memory T cells exhibit higher clonal expansion compared to $CD69^-CD103^-CD8^+$ memory T cells. To analyse the TCR repertoire of SF $CD8^+$ T cells, TCRVβ CDR3 sequencing was performed with sorted $CD45RA^-CD8^+$ T-cell populations. The diversity of CDR3 calculated using Simpson's reciprocal index tended to be lower in the $CD69^+CD103^+CD45RA^-CD8^+$ T-cell population than in the $CD69^-CD103^-CD45RA^-CD8^+$ T-cell population. D50 values, which represent the percentage of unique T-cell clones that account for 50% of the total CDR3 counted, exhibited significantly less diversity in both $CD69^+CD103^+$ and $CD69^+CD103^-CD45RA^-CD8^+$ T cells than in $CD69^-CD103^-CD45RA^-CD8^+$ T cells (Figure 3a).Figure 3b is a representative dataset describing the three subsets from a single patient with RA. The top 10 clones accounted for 60–87% of the $CD69^+CD103^+CD45RA^-CD8^+$ T-cell population and 32–59% of the $CD69^-CD103^-CD45RA^-CD8^+$ T-cell population, indicating a higher degree of skewed cell expansion in the $CD69^+CD103^+CD45RA^-CD8^+$ T-cell population (Figure 3c). An evaluation of CDR3 usage within the total repertoire of sorted $CD8^+$ T-cell subsets showed that $CD69^+CD103^{+/-}$ cells exhibit reduced diversity (Supplementary figure 3a). Furthermore, V-J combination indicated skewing of the T-cell repertoire in $CD69^+CD103^+$ and $CD69^+CD103^-CD8^+$ T-cell populations (Supplementary figure 3b). The analysis of TCR overlap between the subpopulations of SF $CD8^+$ memory T cells revealed greater overlap of the TCR repertoire between $CD69^+CD103^-$ and $CD69^+CD103^+CD45RA^-CD8^+$ T cells than the overlap between $CD69^-CD103^-$ and $CD69^+CD103^+CD45RA^-CD8^+$ T cells, with a similar proportion of unique TCRs within each subpopulation (Supplementary figure 3c and d). Collectively, these results suggest that SF $CD69^+CD103^{+/-}CD8^+$ memory T cells are a distinct population characterised by oligoclonal expansion with a skewed TCR repertoire.

IL-15 activates synovial fluid $CD69^+CD103^{+/-}CD45RA^-CD8^+$ T cells in RA patients

Next, we examined the proliferation and effector functions of SF $CD8^+$ T cells. IL-15 plays a role in the maintenance and activation of T_{RM} cells[27] and is increased in the SF of RA patients.[28] Therefore, we examined the effect of *ex vivo* IL-15 or TCR stimulation on SF $CD8^+$ T cells derived from RA patients. First, we confirmed that SF IL-15

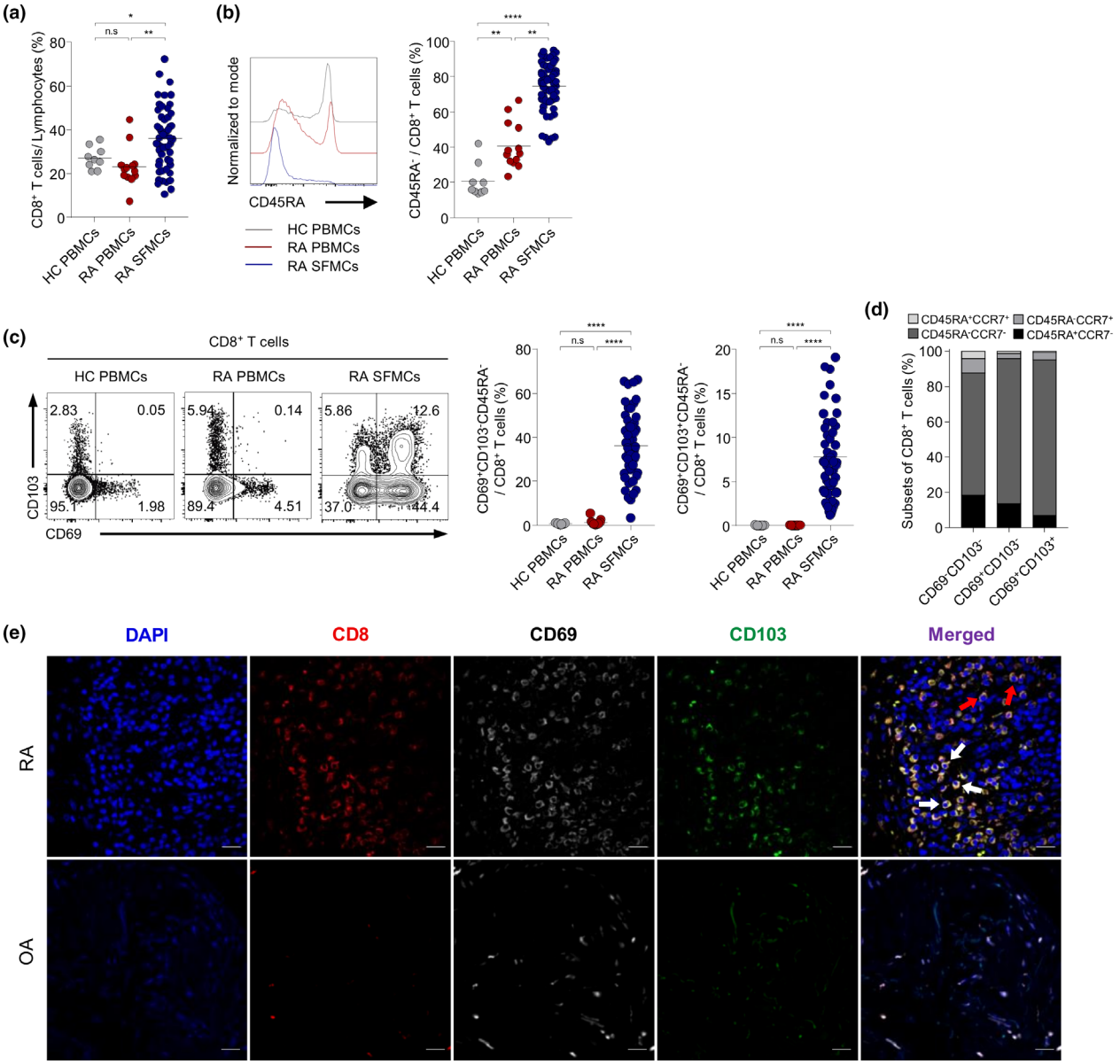

Figure 1. $CD69^{+}CD103^{+/-}CD45RA^{-}CD8^{+}$ T cells are increased in the synovial fluid of RA patients. (**a**) The frequency of $CD8^{+}$ T cells within the lymphocyte population in peripheral mononuclear cells (PBMCs) from healthy controls (HCs; $n = 9$) and rheumatoid arthritis (RA) patients ($n = 13$) and in synovial fluid mononuclear cells (SFMCs) from RA patients ($n = 60$). (**b**) Left: Representative histograms of CD45RA expression in $CD8^{+}$ T cells among PBMCs from HCs and RA patients and SFMCs from RA patients. Right: Dot plot graph depicting the frequency of $CD45RA^{-}CD8^{+}$T cells among PBMCs from HCs ($n = 9$) and RA patients ($n = 13$) and SFMCs from RA patients ($n = 60$). (**c**) Left: Representative flow cytometry plots for CD69 and CD103 expression in $CD45RA^{-}CD8^{+}$ T cells among PBMCs from HCs or RA patients and SFMCs from RA patients. Right: The frequencies of $CD69^{+}CD103^{-}CD45RA^{-}$ and $CD69^{+}CD103^{+}CD45RA^{-}CD8^{+}$ T cells among PBMCs from HCs ($n = 9$) and RA patients ($n = 13$) and SFMCs from RA patients ($n = 60$). (**d**) The proportions of $CD45RA^{+}CCR7^{+}$ (naive), $CD45RA^{-}CCR7^{+}$ (central memory), $CD45RA^{-}CCR7^{-}$ (effector memory) and $CD45RA^{+}CCR7^{-}$ ($CD45RA^{+}$ effector memory) cells among $CD69^{-}CD103^{-}$, $CD69^{+}CD103^{-}$ and $CD69^{+}CD103^{+}CD8^{+}$ T cells from the synovial fluid in patients with RA. (**e**) Representative images of the immunohistochemical staining in synovial tissues from patients with RA and osteoarthritis (OA); red-coloured cells represent CD8, white represent CD69, and green represent CD103. White arrows indicate $CD69^{+}CD103^{+}CD8^{+}$ cells, and red arrows indicate $CD69^{+}CD103^{-}CD8^{+}$ cells. Scale bars = 20μm. Statistical test: one-way ANOVA with Tukey's multiple comparisons test; ***P*-value <0.01, ****P*-value <0.001, *****P*-value <0.0001. Data were obtained from a single experiment for each donor. HC, healthy control; OA, osteoarthritis; PBMC, peripheral blood mononuclear cells; RA, rheumatoid arthritis; SFMC, synovial fluid mononuclear cells.

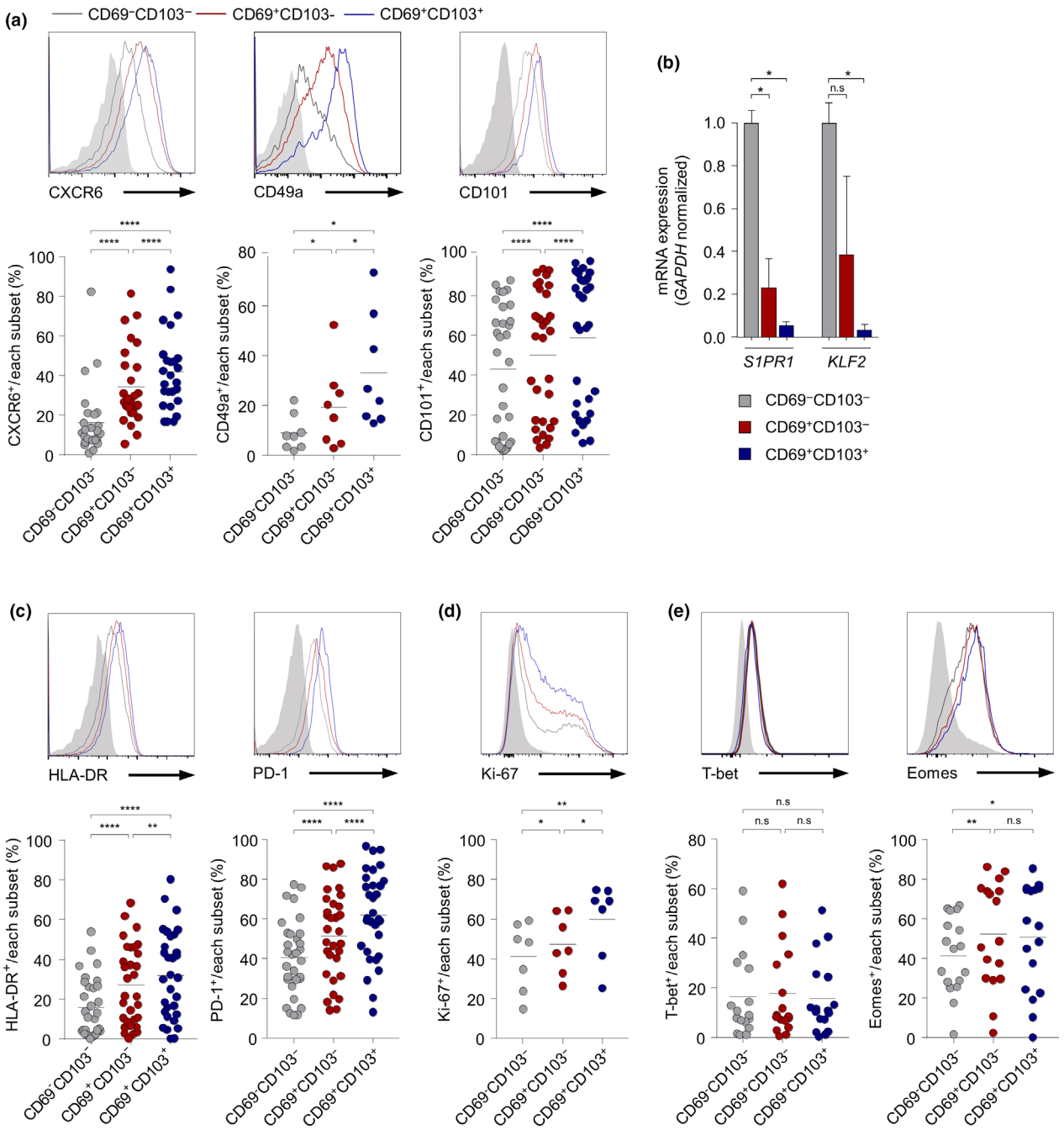

Figure 2. CD69$^+$CD103$^{+/-}$CD45RA$^-$CD8$^+$ T cells from the synovial fluid of patients with RA exhibit T_{RM}-like signatures. **(a)** Upper panel: Representative histograms depicting the expression of the indicated protein on CD69$^-$CD103$^-$ (grey), CD69$^+$CD103$^-$ (red) and CD69$^+$CD103$^+$ (blue) CD45RA$^-$CD8$^+$ T cells among SFMCs from RA patients. The grey-shaded histogram represents the isotype control. Lower panel: Dot plot graphs indicate the frequency of CXCR6, CD49a and CD101 in the indicated subsets among CD45RA$^-$CD8$^+$ T cells. **(b)** The mRNA expression level of S1PR1 and KLF2 from isolated CD69$^-$CD103$^-$, CD69$^+$CD103$^-$ and CD69$^+$CD103$^+$CD45RA$^-$CD8$^+$ T cells in RA SFMCs. Data are presented as mean+SD as data were distributed normally. **(c–e)** The frequency of cells expressing HLA-DR and PD-1 **(c)**, Ki-67 **(d)**, T-bet and Eomes **(e)** was determined and analysed in CD69$^-$CD103$^-$, CD69$^+$CD103$^-$ and CD69$^+$CD103$^+$CD45RA$^-$CD8$^+$ T cells from patients with RA. Statistical test: one-way ANOVA with Tukey's multiple comparisons test; **P*-value <0.05, ***P*-value <0.01, ****P*-value <0.001, *****P*-value <0.0001. Data were obtained from a single experiment for each patient.

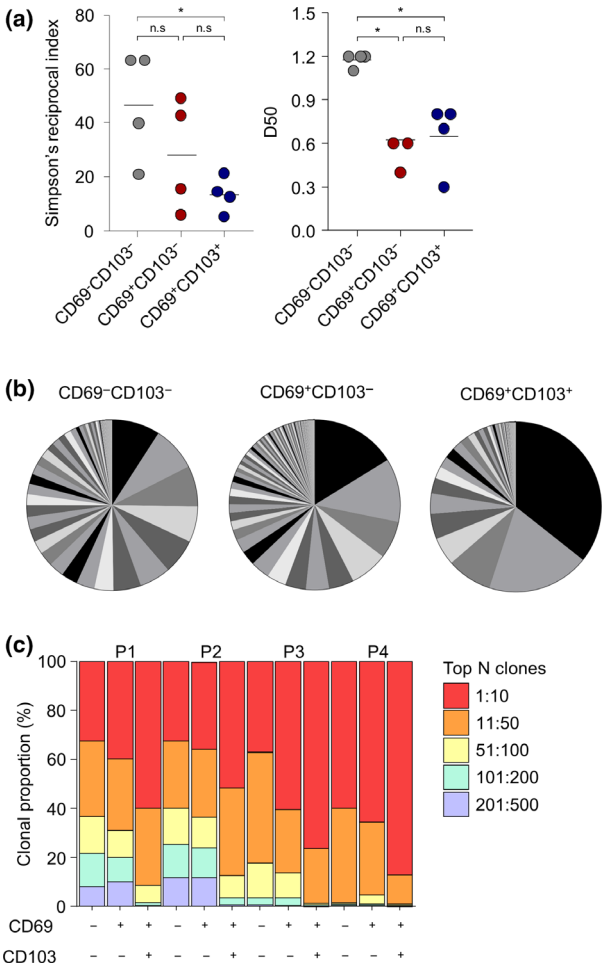

Figure 3. $CD69^+CD103^+CD45RA^-CD8^+$ T cells are a distinct population of cells with skewed TCR repertoires against certain antigens. **(a)** The TCR diversity of isolated SF $CD69^-CD103^-$, $CD69^+CD103^-$ and $CD69^+CD103^+CD45RA^-CD8^+$ T cells was determined using Simpson's reciprocal index (left) and D50 (right), which indicate the percentage of unique T-cell clones that account for the cumulative 50% of the total CDR3 counted. **(b)** Representative data for detected clones with unique CDR3 regions and their frequencies. The graphs represent data from four patients. **(c)** The proportion of top clones with unique CDR3 regions among the total clones of $CD69^-CD103^-$, $CD69^+CD103^-$ and $CD69^+CD103^+CD45RA^-CD8^+$ T cells from the synovial fluid of patients with RA. Statistical test: unpaired Student's *t*-test; ***P*-value <0.01; n.s., not significant.

concentrations were significantly higher in RA patients than in OA patients, whereas IL-2 and IL-7 levels were not significantly different between the two groups (Supplementary figure 4a). IL-15 and IL-15Rα co-localised in fibroblasts and macrophages within the synovial tissue of RA patients, but not the synovial tissue of OA patients. This indicates trans-presentation of IL-15 by IL-15Rα in RA synovial tissues (Supplementary figure 4b). Furthermore, although IL-15Rβ expression was not different between $CD45RA^-CD8^+$ T-cell subsets, CD132 (common γ chain) was upregulated in synovial $CD69^+CD103^{+/-}$ compared to $CD69^-CD103^-CD45RA^-CD8^+$ T cells (Supplementary figure 5). CFSE dilution assays showed that, following IL-15 stimulation, the fold increase in the frequency of $CFSE^{low}$ cells, which were undergoing proliferation, was significantly higher in $CD69^+CD103^+$ and $CD69^+CD103^-CD45RA^-CD8^+$ T cells compared to $CD69^-CD103^-CD45RA^-CD8^+$ T cells (Figure 4a). In contrast, SF $CD8^+$ T cells exhibited comparable rates of proliferation among the subpopulations in response to TCR stimulation.

To determine the function of SF $CD8^+$ T cells with regard to inflammation and cytotoxicity, we examined the production of pro-inflammatory cytokines and cytotoxic molecules after stimulation with IL-15 or anti-CD3 antibodies. Even though IFN-γ and TNF-α were significantly increased by TCR stimulation in all SF $CD45RA^-CD8^+$ T-cell subsets, IL-15 had no significant effect on the production of these pro-inflammatory cytokines (Figure 4b). Without stimulation, perforin and granzyme B were highly expressed in $CD69^+CD103^{+/-}$ $CD45RA^-CD8^+$ T cells compared to $CD69^-CD103^-CD45RA^-CD8^+$ T cells (Figure 4c). The expression of perforin and granzyme B was markedly increased in $CD69^+CD103^-$ and $CD69^+CD103^+CD45RA^-CD8^+$ T cells after stimulation with IL-15 but not anti-CD3 antibodies. These effects of IL-15 on the expression of cytotoxic molecules were not observed in $CD69^-CD103^-CD45RA^-CD8^+$ T cells. Taken together, the results indicate that the SF $CD69^+CD103^{+/-}CD8^+$ memory T cells of RA patients exhibit enhanced proliferation and cytotoxic activities, particularly after IL-15 stimulation.

IL-15-stimulated $CD69^+CD103^{+/-}CD45RA^-CD8^+$ T cells induce perforin-mediated citrullinated histone formation

Given the marked increase in perforin expression upon IL-15 stimulation of $CD69^+CD103^{+/-}CD45RA^-CD8^+$ T cells, we examined their involvement in the pathogenesis of RA. A recent study demonstrated that perforin can induce the citrullination of proteins through NET formation.[29,30] Indeed, high amounts of

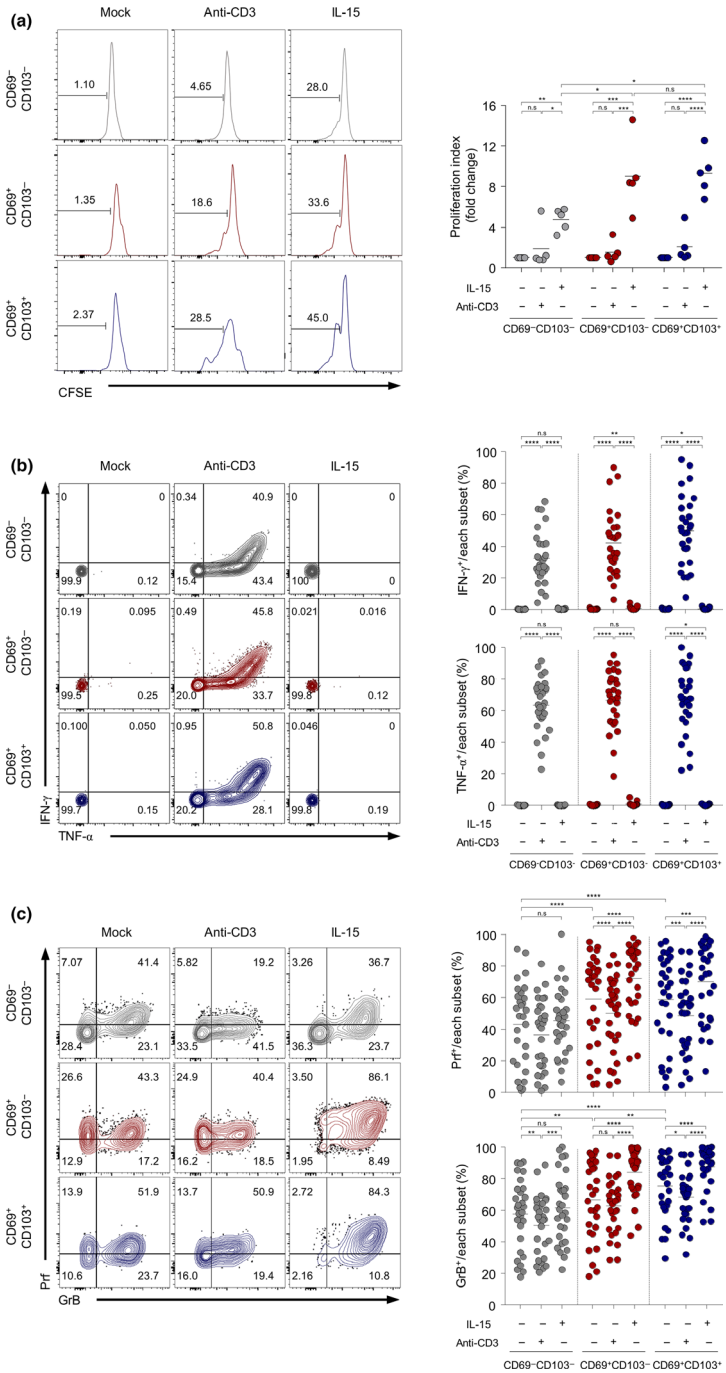

Figure 4. IL-15 stimulation induces increased proliferation and cytotoxic potential in synovial fluid CD69$^+$CD103$^{+/-}$CD45RA$^-$CD8$^+$ T cells. **(a)** Proliferation in response to stimulation with anti-CD3 antibodies or IL-15 was determined by CFSE dilution assay in sorted CD69$^-$CD103$^-$, CD69$^+$CD103$^-$, and CD69$^+$CD103$^+$CD45RA$^-$CD8$^+$ T cells from the synovial fluid of patients with RA (n = 5). The proliferation index represents the fold change (%) in CFSE^{low} cells compared to the mock group. (**b and c)** Pro-inflammatory cytokine expression (**b**) and the expression of cytotoxic effector molecules perforin and granzyme B (**c**) in CD69$^-$CD103$^-$, CD69$^+$CD103$^-$ and CD69$^+$CD103$^+$CD45RA$^-$CD8$^+$ T cells from the synovial fluid of RA patients (n = 29) were analysed after stimulation with or without anti-CD3 antibodies or IL-15. Representative flow cytometry plots are presented on the left. On the right is a comparison of the production of cytokines (**b**) and effector molecules (**c**) between subsets or stimulations. Statistical test: one-way ANOVA with Tukey's multiple comparisons test; *P-value <0.05, **P-value <0.01, ****P-value <0.0001. Data were obtained from a single experiment for each patient. CFSE, carboxyfluorescein succinimidyl ester; Prf, perforin; GrB, granzyme B.

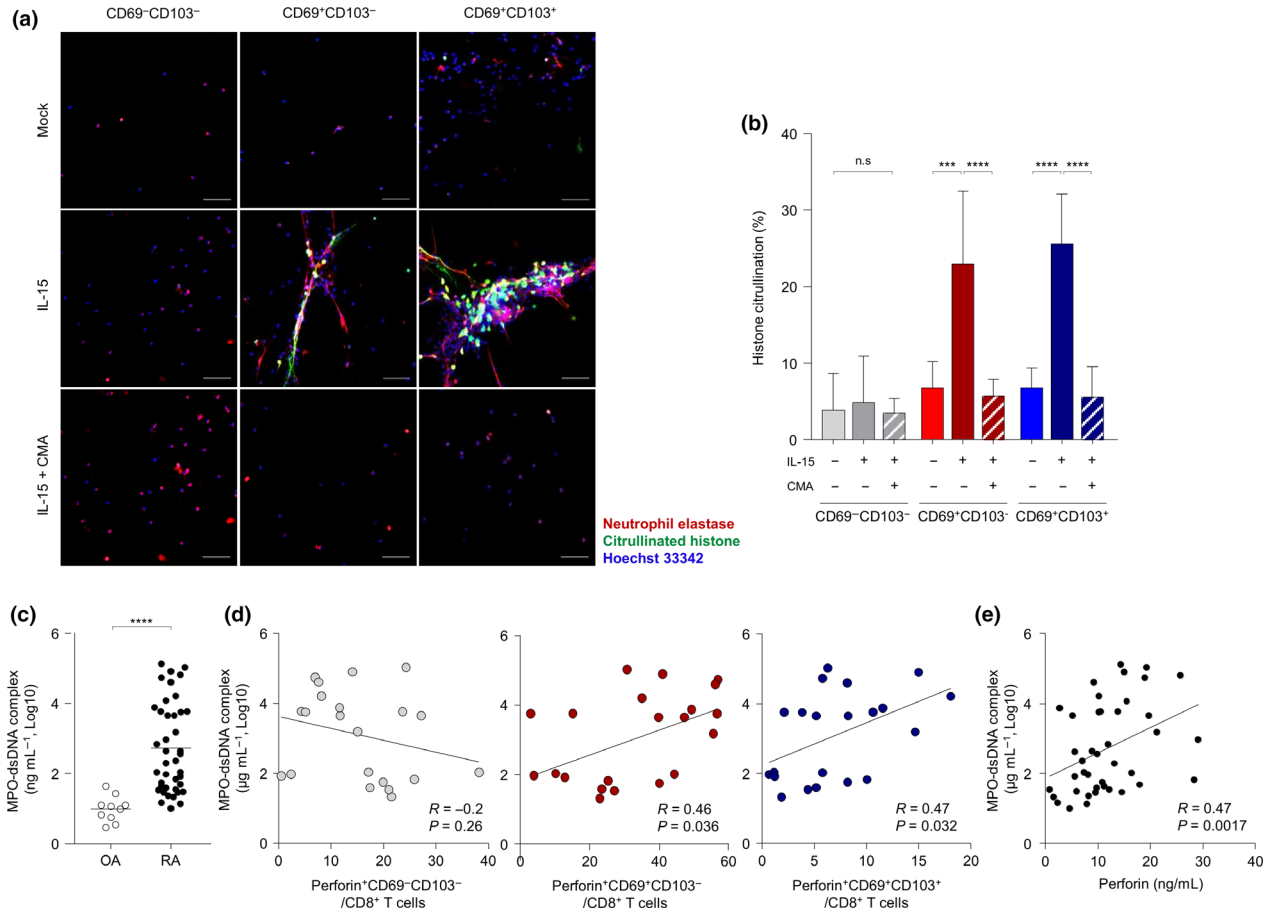

Figure 5. IL-15-stimulated synovial $CD69^+CD103^-$ and $CD69^+CD103^+CD45RA^-CD8^+$ T cells induce perforin-mediated citrullination in freshly isolated, healthy neutrophils. **(a)** $CD69^-CD103^-$, $CD69^+CD103^-$ and $CD69^+CD103^+CD45RA^-CD8^+$ T cells were sorted, pre-incubated with or without CMA, and stimulated with IL-15 (20ngmL^{-1}) for 48h. The supernatants from each subset were added to freshly isolated neutrophils from a healthy donor. Neutrophils undergoing histone citrullination were visualised by immunofluorescent confocal microscopy using antibodies against citrullinated histones with FITC (green), neutrophil elastase with Alexa Fluor 647 (red), and DNA-binding Hoechst 33342 (blue). Scale bars=20μm. **(b)** The levels of histone citrullination were measured under the indicated conditions using ImageJ from at least five images. **(c)** Concentration of MPO-dsDNA complex in synovial fluid of OA (n=11) and RA (n=42) patients. **(d)** Correlation between perforin-expressing $CD69^-CD103^-$, $CD69^+CD103^-$ and $CD69^+CD103^+$ cells among $CD8^+$ T cells with levels of MPO-dsDNA complex in synovial fluid of RA patients. **(e)** Correlation between the concentration of perforin and MPO-dsDNA complex in synovial fluid of RA patients (n=42). Data are presented as mean+SD as data were distributed normally. Statistical tests: one-way ANOVA with Tukey's multiple comparisons test **(b)**, unpaired Student's t-test **(c)** and Spearman's rank correlation analysis **(d and e)**; **P-value <0.01, ****P-value <0.0001. CMA, concanamycin A; MPO-dsDNA, myeloperoxidase-double-stranded DNA; OA, osteoarthritis; RA, rheumatoid arthritis.

citrullinated histones were produced in perforin-treated neutrophils and were comparable to ionomycin-treated neutrophils; such effects were not observed following incubation with calcium-chelating agent EGTA (Supplementary figure 6a). Next, we treated neutrophils with supernatants harvested from the sorted peripheral blood $CD45RA^-CD8^+$ T cells of healthy controls and RA patients cultured with or without IL-15. Citrullinated histones were significantly increased when neutrophils were treated with supernatants from IL-15-stimulated peripheral blood $CD45RA^-CD8^+$ T cells, but without NET formation (Supplementary figure 6b). Importantly, supernatants from IL-15-stimulated SF $CD69^+CD103^-$ or $CD69^+CD103^+CD45RA^-CD8^+$ T cells induced histone citrullination along with the formation of NET, allowing citrullinated proteins to be secreted into the extracellular space (Figure 5a and b). This effect was abolished when $CD8^+$ T cells were pre-incubated with perforin-inhibitor concanamycin A (CMA),[31] indicating that

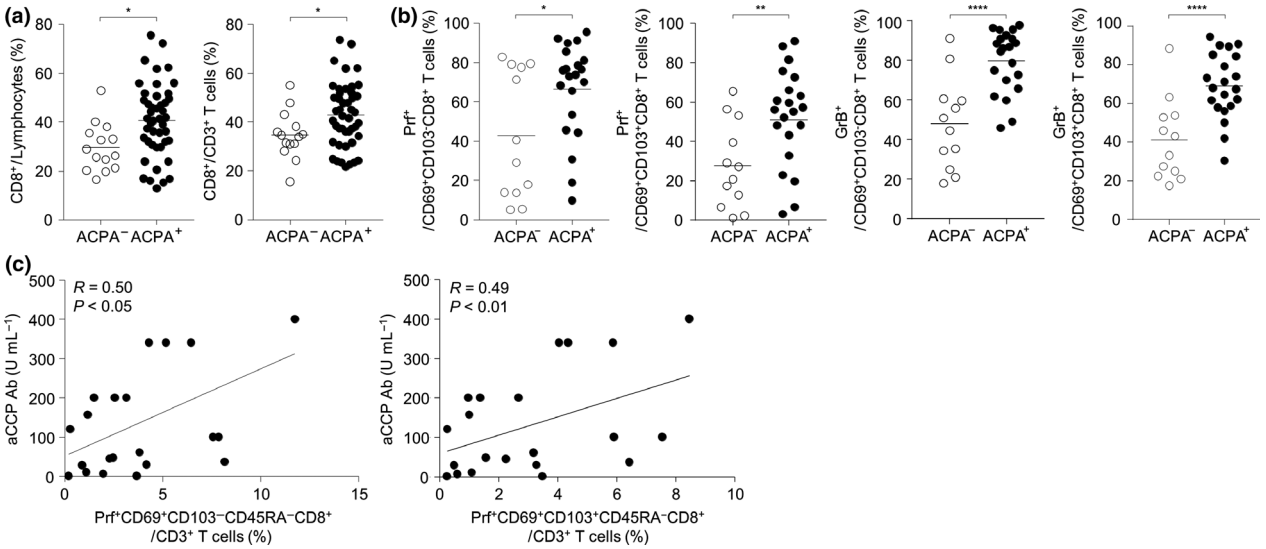

Figure 6. ACPA-positive patients have an increased frequency of synovial CD8$^+$ memory T cells with more cytotoxic effector molecules than ACPA-negative patients. **(a)** Quantitation of the proportion of CD8T cells within synovial lymphocytes and CD3$^+$ T cells in ACPA-negative (n = 14) and ACPA-positive (n = 45) patients. **(b)** The frequency of cells expressing perforin or granzyme B among synovial CD69$^+$CD103$^-$ and CD69$^+$CD103$^+$CD45RA$^-$CD8$^+$ T cells in ACPA-negative (n = 12) and ACPA-positive (n = 21) patients. **(c)** Correlation between the anti-cyclic citrullinated protein antibody titre and the frequency of perforin-expressing CD69$^+$CD103$^-$CD45RA$^-$CD8$^+$ (left) or CD69$^+$CD103$^+$CD45RA$^-$CD8$^+$ T cells (right) in RA patients with ACPA (n = 21). Statistical tests: unpaired Student's t-test **(a and b)** and Spearman's rank correlation analysis **(c)**; *P-value <0.05, **P-value <0.01, ***P-value <0.001. ACPA, anti-citrullinated protein antibody; aCCP, anti-cyclic citrullinated peptide antibodies; Prf, perforin; GrB, granzyme B.

perforin is responsible for the citrullination with the process of NET formation. Furthermore, MPO-dsDNA complex levels, which indicate NET release, were significantly higher in the SF of RA patients than in that of OA patients (Figure 5c). The frequency of perforin-expressing CD69$^+$CD103$^-$ or CD69$^+$CD103$^+$CD45RA$^-$CD8$^+$ T cells in SF correlated with the levels of MPO-dsDNA complex (Figure 5d). Interestingly, perforin levels in the SF correlated with the concentrations of MPO-dsDNA complex (Figure 5e). Furthermore, perforin-expressing CD8$^+$ T cells were located near citrullinated histones in the synovial tissue of RA patients (Supplementary figure 7). Overall, these data indicate that IL-15-stimulated CD69$^+$CD103$^{+/-}$CD8$^+$ memory T cells induce perforin-mediated histone citrullination with the formation of NET complex.

Perforin-expressing CD69$^+$CD103$^{+/-}$CD45RA$^-$CD8$^+$ T cells are associated with ACPA-positive RA

Finally, we analysed the implication of CD69$^+$CD103$^{+/-}$CD8$^+$ T cells in RA, particularly ACPA-positive RA. The frequency of CD8$^+$ T cells among lymphocyte or CD3$^+$ T-cell-gated SFMCs was significantly higher in ACPA-positive patients than in ACPA-negative patients (Figure 6a). Furthermore, the frequency of perforin-expressing cells among CD69$^+$CD103$^-$ or CD69$^+$CD103$^+$CD45RA$^-$CD8$^+$ T cells was significantly higher in ACPA-positive patients than in ACPA-negative patients (Figure 6b). A similar result was obtained when the frequency of granzyme B-expressing cells was analysed (Figure 6b). Importantly, the frequency of perforin-expressing CD69$^+$CD103$^-$CD8$^+$ or perforin-expressing CD69$^+$CD103$^+$CD8$^+$ T cells among CD3$^+$ T cells significantly correlated with the ACPA titre in the serum of ACPA-positive RA patients (Figure 6c). The frequency of perforin-expressing CD69$^+$CD103$^{+/-}$CD45RA$^-$CD8$^+$ T cells among CD3$^+$ T cells did not correlate with DAS28 levels in ACPA-positive patients (Supplementary figure 8). Taken together, these findings indicate that perforin-expressing CD69$^+$CD103$^{+/-}$CD8$^+$ memory T cells are associated with the citrullination and production of ACPA.

DISCUSSION

In the present study, we demonstrated that the SF CD69$^+$CD103$^{+/-}$CD8$^+$ memory T cells of RA patients

exhibit the phenotype of tissue-resident cells with effector-like features. Moreover, a TCR repertoire analysis revealed less TCR diversity in the $CD69^+CD103^{+/-}$ cell population, with skewed TCR usage. In addition, IL-15 stimulation of $CD69^+CD103^{+/-}CD45RA^-CD8^+$ T cells not only increased the expression of cytotoxic molecules, but induced the citrullination of histones with formation of NETs in a perforin-dependent manner. Furthermore, perforin-expressing $CD69^+CD103^{+/-}CD45RA^-CD8^+$ T cells were enriched in the SF of ACPA-positive patients, and their frequency correlated with the SF MPO-dsDNA complex level and ACPA titre.

An analysis of synovial immune cells from RA patients provided evidence for the involvement of T cells in the pathogenesis of RA. Previous studies have focused on the pathogenic role of pro-inflammatory cytokines, such as TNF-α and IL-17A. TCR analysis showed that expanded circulating T cells with signatures of pro-inflammatory cytokine production and synovium infiltration are present in autoimmune arthritis.[32,33] A few studies have highlighted the possible influence of $CD8^+$ T cells in RA,[9-11] and a strong association between RA and MHC class I polymorphisms.[34] However, detailed phenotypes and functions, especially within specific subsets of $CD8^+$ T cells, including T_{RM} cells, have not been studied in RA. In the present study, we examined the SF $CD8^+$ T cells of RA patients to determine whether these cells contribute to the pathogenesis of the disease.

We found that expanded SF $CD8^+$ T cells contain $CD69^+CD103^+$ and $CD69^+CD103^-$ cells. CD69 and CD103 are considered canonical markers of T_{RM} cells, which can participate not only in protection against pathogens and tumors, but also in the pathogenesis of autoimmune disorders.[15,20,21,35-37] In response to IL-15, autoreactive T_{RM} cells can contribute to autoimmune skin diseases, such as vitiligo.[38] Our present study revealed that SF $CD69^+CD103^{+/-}CD45RA^-CD8^+$ T cells exhibit characteristics of T_{RM} cells; they downregulated the mRNA expression of S1PR1, which is critical for recirculation through the detection of S1P in blood and lymph nodes, and its transcription regulator KLF2. We also found that SF $CD69^+CD103^{+/-}CD45RA^-CD8^+$ T cells express significantly higher levels of PD-1 and CD101, which are upregulated in T_{RM} cells, than $CD69^-CD103^-CD45RA^-CD8^+$ T cells in RA patients. The increased expression of PD-1 and memory marker Eomes, but not activation markers CD25 and CD38, suggests that these cells are not merely activated T cells, but rather differentiated effector or memory cells. These findings indicate that SF $CD69^+CD103^{+/-}CD8^+$ memory T cells in RA exhibit features of T_{RM} cells. However, SF is an exudate, rather than an inflamed tissue, and the tissue residency of $CD69^+CD8^+$ T cells was not assessed directly. In addition, considering that activation marker HLA-DR was upregulated in $CD69^+CD103^{+/-}CD45RA^-CD8^+$ T cells, and an increase in cytotoxic molecules in response to IL-15 could be a feature of $CD8^+$ memory T cells, we cannot rule out the possibility that SF $CD69^+CD103^{+/-}CD8^+$ T cells were memory or activated T cells rather than T_{RM} cells. Therefore, further studies including functional analysis of tissue residency are required to confirm that these cells are bona fide T_{RM} cells.

Although similar expression patterns of T_{RM} markers were observed in both $CD69^+CD103^+$ and $CD69^+CD103^-$ subsets, the degree of expression was different between the two subsets. The expression of chemokine receptor CXCR6 and adhesion protein CD49a was significantly higher in $CD69^+CD103^+$ cells than $CD69^+CD103^-$ cells. In addition, the frequencies of PD-1^+ and $CD101^+$ cells were higher in $CD69^+CD103^+$ cells than $CD69^+CD103^-$ cells, suggesting that $CD69^+CD103^+$ cells were a distinct population more closely resembling T_{RM} cells. The decreased diversity and skewing of the TCRVβ CDR3 repertoire were profound in $CD69^+CD103^+$ cells, whereas $CD69^+CD103^-$ cells exhibited a mild contraction of the repertoire compared to $CD69^-CD103^-CD45RA^-CD8^+$ T cells. However, the shared TCR repertoire between $CD69^+CD103^-$ and $CD69^+CD103^+CD45RA^-CD8^+$ T cells suggests that two subpopulations may have originated from the same predecessors. In contrast, $CD69^-CD103^-$ cells exhibited less overlap with $CD69^+CD103^+CD45RA^-CD8^+$ T cells. Further studies designed to distinguish between the two subpopulations within $CD69^+CD8^+$ T cells would contribute to understanding immune responses during joint inflammation.

IL-15 has been considered an indispensable cytokine for the development, homeostasis and survival of T_{RM} cells in peripheral tissues.[14,27] The present study confirms higher levels of SF IL-15 in RA patients than in OA patients as reported in a previous study.[28] In addition, we observed that IL-15 co-localised with IL-15Rα in fibroblasts and macrophages from the synovial tissues of RA

patients, signifying trans-presentation of IL-15. The proliferation and expression of cytotoxic molecules were significantly increased by IL-15 in SF CD8$^+$ T cells, particularly CD69$^+$CD103$^{+/-}$ subsets. The increased expression of CD132 may explain the augmented response to IL-15 stimulation by SF CD69$^+$CD103$^-$ and CD69$^+$CD103$^+$CD45RA$^-$CD8$^+$ T cells. Interestingly, IL-15 stimulation also induced an increase in cytotoxic molecule expression in CD69$^+$CD45RA$^-$CD8$^+$ T cells from the peripheral blood of HC or RA patients (data not shown); thus, the response to IL-15 is a general feature of CD69$^+$CD8$^+$ memory T cells. Considering the increased IL-15 concentration and its general effect on CD69$^+$CD45RA$^-$CD8$^+$ T cells, especially on CD69$^+$CD103$^{+/-}$ subsets, the role of IL-15 in the pathophysiology of RA should be studied further.

Citrullination and the presence of antibodies against to citrullinated proteins is one of the hallmarks in the pathogenesis of RA. Because NET complex contains citrullinated histones,[26] it can be a source of citrullinated autoantigens.[28] The activation of peptidylarginine deiminases, enzymes responsible for protein citrullination, is mediated by an influx of calcium ions into the cytosol of neutrophils. This leads to the formation of numerous citrullinated proteins, including histones.[28,39] Because perforin is a pore-forming agent in the cell membrane and allows for the influx of calcium ions into target cells, it can generate citrullinated proteins in RA.[28] In the present study, we found that IL-15-stimulated CD69$^+$CD103$^{+/-}$CD8$^+$ memory T cells can induce neutrophil histone citrullination and the release of neutrophil elastase into the extracellular space in the process of NET formation. The frequency of perforin-expressing CD69$^+$CD103$^-$ or CD69$^+$CD103$^+$CD45RA$^-$CD8$^+$ T cells significantly correlated with the levels of MPO-dsDNA complex. Importantly, the expression of perforin was higher in SF CD69$^+$CD103$^{+/-}$CD45RA$^-$CD8$^+$ T cells from ACPA-positive RA patients than those from ACPA-negative patients and correlated with the ACPA titre. These findings suggest that CD69$^+$CD103$^{+/-}$ subsets of SF CD8$^+$ T cells may be a major trigger for citrullinated protein formation. Therefore, they likely play a role in the pathogenesis of RA, particularly in patients with ACPA-positive RA.

In conclusion, our data indicate that expanded SF CD8$^+$ memory T cells from RA patients contain CD69$^+$CD103$^{+/-}$ subsets that exhibit phenotypes of canonical T_{RM} cells with effector-like features. CD69$^+$CD103$^{+/-}$ cells are more responsive to IL-15, which was detected in the SF and tissue of patients with RA, and exhibit increased proliferation and cytotoxic potential. Furthermore, IL-15-stimulated CD69$^+$CD103$^{+/-}$CD45RA$^-$CD8$^+$ T cells induce perforin-mediated histone citrullination and NET formation. We also demonstrated that synovial perforin-expressing CD69$^+$CD103$^{+/-}$CD45RA$^-$CD8$^+$ T cells are associated with ACPA-positive RA. Taken together, our data suggest that SF CD69$^+$CD103$^{+/-}$CD8$^+$ memory T cells with T_{RM} features play a role in the pathogenesis of ACPA-positive RA by inducing perforin-mediated citrullinated protein formation.

METHODS

Patients and samples

SF samples were obtained from 60 patients diagnosed with RA at Asan Medical Center (Seoul, Korea). All patients had active disease at the time of sampling, for which they required joint aspiration with or without intraarticular injection of corticosteroids. For immunofluorescence, synovial tissues were acquired from the synovium of OA and RA patients who underwent arthroplasty or synovectomy. The diagnosis of RA was based on the 2010 revised American College of Rheumatology/European League Against Rheumatism criteria for the classification of RA. The clinical and demographic data of studied patients are summarised in Supplementary table 1.

Reagents and antibodies

The following monoclonal antibodies were used for multicolour flow cytometric analysis: anti-CD3 (UCHT1), anti-CD8 (HIT-8a), anti-CD38 (HIT2), anti-CD45RA (HI100), anti-CD49a (SR84) and anti-CD132 (AG184) from BD Biosciences (San Jose, CA, USA); anti-CD8 (T8, Leu2), anti-CD25 (BC96), anti-CD69 (FN50), anti-CD101 (BB27), anti-CD103 (Ber-ACT8), anti-CXCR6 (K041E5), anti-granzyme B (QA16A02), anti-IFN-γ (4S.B3), anti-IL-15Rβ (TU27), anti-perforin (B-D48), anti-TCR$\gamma\delta$ (B1) and anti-TNF-α (MAb11) from BioLegend (San Diego, CA, USA); anti-CD14 (61D3), anti-CD19 (HIB19), anti-CD56 (CMSSB), anti-Ki-67 (20Raj1), anti-T-bet (eBio4B10) and Fixable Viability Dye eFluor® 506 from eBioscience (San Diego, CA, USA); and anti-Eomes (WD1928) from Invitrogen (Carlsbad, CA, USA). For immunofluorescent staining of synovial tissues and NET formation, anti-CD8 (YTC182.20), monoclonal anti-IL-15, polyclonal anti-CD68, anti-CD103 (EPR4166(2)) and anti-histone H3 (citrulline R2 + R8 + R17) antibodies were obtained from Abcam (Cambridge, UK). Anti-CD69 (FN50), anti-CD55/DAF, anti-IL-15Rα and anti-neutrophil elastase (NP57) were obtained from BioLegend, Novus Biologicals (Littleton, CO, USA), R&D Systems (Minneapolis, MN, USA) and Santa Cruz (Santa Cruz, CA, USA), respectively. Recombinant human IL-15 (PeproTech, Rocky Hill, NJ, USA) was used for the stimulation of SFMCs and sorted CD8$^+$ T cells. The concentrations of IL-15, IL-2, IL-7 and perforin in

the SF were measured by enzyme-linked immunosorbent assay (ELISA) using DuoSet (R&D Systems) and ELISA Set (Abcam) according to the manufacturers' instructions.

Mononuclear cell isolation and stimulation

SF samples were collected by centrifugation at 1800 g for 10 min. The supernatants were stored at −80°C until cytokine measurement. Pellets from the SF and peripheral blood were subjected to density gradient centrifugation using Ficoll-Paque™ PLUS (GE Healthcare, Piscataway, NJ, USA) to isolate mononuclear cells. Cells were cryopreserved using FBS (Welgene, Daejeon, South Korea) supplemented with 10% dimethyl sulfoxide (DMSO; Sigma Aldrich, St. Louis, MO, USA) and stored in liquid nitrogen until thawed for further usage. To determine the production of pro-inflammatory cytokines and cytotoxic effector molecules, isolated mononuclear cells were incubated in RPMI 1640 medium (Welgene) supplemented with 10% FBS (Welgene) and 1% penicillin and streptomycin (P/S) (Welgene) in the presence or absence of rhIL-15 (20 ng mL^{-1}) for 24 h at 37°C in a 5% CO_2 atmosphere. When indicated, anti-CD3 antibodies (1 μg mL^{-1}; BD Biosciences), brefeldin A (GolgiStop™; BD Biosciences) and monensin (GolgiPlug™; BD Biosciences) were added in the last 5 h of the incubation.

Flow cytometric analysis

Cryopreserved SFMCs and PBMCs were thawed at 37°C and incubated with Fixable Viability Dye eFluor® 506 (eBioscience) for 20 min at 4°C without light exposure according to the manufacturer's instructions to exclude dead cells. The cells were then washed with DPBS containing 1% FBS (Welgene) and 0.05% sodium azide and subsequently stained with fluorochrome-conjugated antibodies against surface proteins or fluorochrome-matched isotype controls for 30 min at 4°C. For the staining of intracellular proteins, surface-stained cells were fixed and permeabilised using the FoxP3 Staining Buffer Kit (eBioscience) according to the manufacturer's instructions. The cells were stained with antibodies against intracellular proteins and matched isotype controls for 30 min at 4°C. After washing, samples were acquired on a BD FACSCanto™ II flow cytometer (BD Biosciences) and analysed using FlowJo software (TreeStar, Ashland, OR, USA).

Cell sorting

$CD45RA^-CD8^+$ T-cell subsets were isolated according to the expression of CD69 and CD103. Cryopreserved SFMCs were thawed and washed with DPBS (Welgene) containing 2% FBS (Welgene) and 2 mM EDTA (Sigma Aldrich). $CD8^+$ T cells were magnetically separated from RA SFMCs using the $CD8^+$ T Cell Isolation Kit (Miltenyi Biotec, Auburn, CA, USA). $CD8^+$ T cells were stained with Fixable Viability Dye eFluor® 506 (eBioscience) and surface antibodies, filtered and further sorted into $CD69^-CD103^-$, $CD69^+CD103^-$ and $CD69^+CD103^+CD45RA^-CD8^+$ subsets using FACSARIA™ III (BD Biosciences).

Quantitative RT-PCR

Total RNA was extracted from the sorted $CD69^{+/-}CD103^{+/-}CD45RA^-CD8^+$ T cells from the RA SFMCs using TRIzol (Invitrogen), and extracted RNA was reverse-transcribed into cDNA using the SuperScript™ IV First-Strand Synthesis System (Invitrogen) according to the manufacturer's instructions. Quantitative PCR (qPCR) was performed with TOPreal™ qPCR 2X PreMIX (SYBR Green with low ROX; Enzynomics, Daejeon, South Korea) on a LightCycler® 480 Instrument II (Roche, Branchburg, NJ, USA). Custom-designed primers (Cosmogenetech, Seoul, South Korea) were used (Supplementary table 2). The RNA expression levels were determined based on the normalisation of the relative expression of target genes to the control gene *GAPDH*.

TCR sequencing

A total of 15,000-550,000 $CD69^-CD103^-$, $CD69^+CD103^-$ and $CD69^+CD103^+CD45RA^-CD8^+$ T cells from RA SFMCs were sorted and analysed (details about the cell and sequencing data are presented in Supplementary table 3). Dead cells were excluded from sorting using Fixable Viability Dye eFluor® 506 (eBioscience). The cells were collected and stored in RNAlater™ Stabilization Solution (Thermo Fisher Scientific, Waltham, MA, USA) at −80°C. Total RNA was extracted from the samples using the RNeasy Mini Kit (Qiagen, Hilden, Germany) according to the manufacturer's instructions. cDNA was synthesised using the OneStep RT-PCR Kit (Qiagen) with barcoded primers (iRepertoire, Huntsville, AL, USA). The resulting barcoded cDNA libraries were rescued with SPRIselect beads (Beckman Coulter, Brea, CA, USA) according to the manufacturer's instructions to increase the CDR3 discovery rate and library quality. After bead clean-up, rescued cDNA libraries were amplified exponentially using universal sequencing primers (iRepertoire) and GoTaq G2 Hot Start Master Mix (Promega, Fitchburg, WI, USA). Using NanoDrop 8000 (Thermo Fisher Scientific), the library amplification was regarded as successful if the concentration of the samples was ≥10 ng μL^{-1}. Libraries with unique barcodes were pooled and subjected to quality control by KAPA qPCR. Next-generation sequencing was performed on the Illumina MiSeq system for 600 cycles, and the data were analysed by iRepertoire software. The output data files were used to calculate the D50, which is the percent of top dominant and unique T-cell clones that account for the cumulative 50% of the total CDR3s counted within sample. Simpson's reciprocal index was calculated as follows:

$$D = \frac{N(N-1)}{\Sigma n(n-1)}$$

where D = Simpson's reciprocal index, N = total number of all sequences and n = total number of particular sequences. Simpson's reciprocal index approaching 1 indicates monoclonality, whereas a higher index value represents greater diversity of clonality. Circos plots were produced using the Circos software package.

Proliferation assay

Sorted cells were first labelled using the CellTrace™ CFSE Cell Proliferation Kit (Invitrogen). CFSE-labelled cells were cultured in RPMI 1640 medium with 10% FBS and 1% P/S with or without anti-CD3 antibodies (1 μg mL^{-1}; BD Biosciences) or rhIL-15 (20 ng mL^{-1}, PeproTech) for 48 h at 37°C in a 5% CO_2 atmosphere. After incubation, the cells were harvested and stained with fluorochrome-conjugated antibodies against surface proteins. After washing, samples were acquired on a BD FACSCanto™ II flow cytometer (BD Biosciences) and the frequency of $CFSE^{low}$ cells was determined using FlowJo software (TreeStar).

Neutrophil isolation and NET induction

Peripheral blood from healthy subjects was diluted in DPBS and centrifuged with Ficoll-Paque™ PLUS (GE Healthcare) for density gradient separation. The supernatant including the mononuclear cell layer was removed, and the pellet at the bottom of the tube was resuspended in HBSS without phenol (Welgene). The cells were then added to an equal volume of 3% dextran (MP Biomedicals, Santa Ana, CA, USA) in HBSS and incubated for 30 min at room temperature for erythrocyte sedimentation. The upper layer containing neutrophils was transferred to a new tube and washed. The remaining erythrocytes were lysed using hypotonic lysis buffer and re-equilibration buffer.[40] The cells were washed with HBSS before further analysis. The purity of isolated neutrophils was >90% based on CD66b and CD16 expression as assessed by flow cytometry.

To induce and visualise NET formation, 1.0×10^5 neutrophils were attached to the surface of poly-D-lysine (Thermo Fisher Scientific) coated 12 mm cover glasses (Marienfeld, Lauda-Königshofen, Germany) for 30 min at 37°C. The cells were then stimulated with 5 μm ionomycin (Thermo Fisher Scientific), 500 ng mL^{-1} perforin (Enzo, Farmingdale, NY, USA) or the supernatants of $CD69^{+/-}CD103^{+/-}CD45RA^-CD8^+$ T-cell subsets cultured with or without IL-15 and pre-incubated with 30 nM CMA (Sigma Aldrich) for 2 h when required. For the inhibition of NET formation, the samples were treated with 8 mM EGTA.

Histone citrullination and NET formation

Neutrophils on coated cover glasses were fixed using paraformaldehyde at a final concentration of 4%. Cover glasses were removed from the 24-well plate and washed with DPBS. The cells were permeabilised with PBS + Tween-20 (Bio Basic, Markham, ON, Canada) and blocked with 5% donkey serum in 0.1% PBST for 1 h at room temperature. Citrullinated histones and NETs were stained with rabbit polyclonal anti-histone H3 (R2 + R7 + R18) (1:250) and mouse anti-neutrophil elastase (1:250). Coverslips were washed and stained with donkey-raised anti-rabbit FITC and anti-mouse Alexa Fluor 647 antibodies. DNA was counterstained with Hoechst 33342 (Invitrogen). Citrullinated histones and NETs were visualised using the LSM 710 confocal microscope (Carl Zeiss, Göttingen, Germany). A minimum of five images per slide were taken using the 10× lens in different areas of each coverslip to ensure accurate representation. Digital images were acquired by ZEN software (Carl Zeiss) and analysed using ImageJ software (NIH, Bethesda, MD, USA).

Immunofluorescence microscopy

Synovial tissues were serially cut into sections and embedded with paraffin using microscope cover glasses. For immunofluorescent staining, tissue sections were deparaffinised and rehydrated with xylene and ethanol. The sections were immersed in antigen retrieval solution (Agilent, Santa Clara, CA, USA) citrate buffer (pH 6) and incubated in a microwave for 20 min. The slides were allowed to cool at room temperature for 30 min before washing with DPBS. Next, the slides were blocked with 1% BSA in TBS+ 0.2% Triton X-100 (Bio Basic). The sectioned tissues were stained with the following cocktails of primary antibodies in blocking buffer overnight at 4°C: rat anti-CD8 (1:100), mouse anti-CD69 (1:100) and rabbit anti-CD103 (1:100); mouse anti-IL-15 (1:400), goat anti-IL-15Rα (1:400), rabbit anti-CD55/DAF (1:50) and/or rabbit anti-CD68 (1:50); or rat anti-CD8 (1:100), mouse anti-perforin (1:50) and rabbit anti-histone H3 (R2 + R7 + R18)(1:50). Subsequently, the sections were washed and stained for 1 h at room temperature with the following donkey-raised secondary antibodies: anti-mouse Alexa Fluor 647 (1:500), anti-goat Cy3/Cy5 (1:500), anti-rabbit FITC (1:500) and anti-rat Cy3/Cy5 (1:500). After washing, sections were counterstained with Hoechst 33342 (Invitrogen) and mounted using ProLong Gold Antifade Mountant (Invitrogen).

MPO-dsDNA complex measurement

96-well ELISA microplates were coated with mouse anti-human MPO (clone 4A4; Invitrogen) (1:2000) overnight at 4°C. After washing, the plate was blocked with 1% BSA in PBS. Samples diluted in blocking buffer were treated with DNase (Worthington, Columbus, OH, USA) for 15 min at room temperature to remove unbound DNA followed by EDTA treatment. Samples were then loaded onto plates and incubated overnight at 4°C. Plates were washed and added with diluted Picogreen reagent (1:200) in TE buffer. After incubation for 5 min, fluorescence was measured in Victor X4 (Perkin Elmer, Hopkinton, MA, USA). The concentrations of MPO-dsDNA complex were interpolated from standard curve generated from Quant-iT™ PicoGreen™ dsDNA Assay Kit (Invitrogen).

Statistical analysis

Statistical analyses were performed in Prism7 (GraphPad Software, San Diego, CA, USA). All data are presented as the mean±standard deviation. ACPA-negative and ACPA-positive patients were compared by the Mann–Whitney *U*-test. Correlation studies were performed by Spearman's rank correlation analysis. Comparisons of multiple groups, including healthy controls, RA PBMCs and RA SFMCs, and between the subsets of $CD45RA^-CD8^+$ T cells, were performed by the Student's *t*-test or ANOVA and Tukey's multiple comparisons test. Significance is reported as $P<0.05$.

ACKNOWLEDGMENTS

This research was supported by the Bio & Medical Technology Development Program of the National Research Foundation (NRF) and funded by the Korean government (MSIT) (No. 2018M3A9D3079500).

CONFLICT OF INTEREST

The authors declare no conflict of interest.

AUTHOR CONTRIBUTIONS

JJ, E-CS and SH designed the research. JJ, JSL and SH performed the experiments. JJ, Y-GK, C-KL, BY, E-CS and SH analysed the data. JSL, Y-GK, C-KL, BY and SH provided the clinical samples. JJ, E-CS and SH wrote the manuscript.

ETHICAL APPROVAL

All patients and healthy controls provided written informed consent. The protocols of this study were approved by the Institutional Review Board of Asan Medical Center (2017-0866).

REFERENCES

1. McInnes IB, Schett G. The pathogenesis of rheumatoid arthritis. *N Engl J Med* 2011; **365**: 2205–2219.
2. Malmstrom V, Catrina AI, Klareskog L. The immunopathogenesis of seropositive rheumatoid arthritis: from triggering to targeting. *Nat Rev Immunol* 2017; **17**: 60–75.
3. Yamada H, Nakashima Y, Okazaki K *et al*. Th1 but not Th17 cells predominate in the joints of patients with rheumatoid arthritis. *Ann Rheum Dis* 2008; **67**: 1299–1304.
4. Zhang L, Li YG, Li YH *et al*. Increased frequencies of Th22 cells as well as Th17 cells in the peripheral blood of patients with ankylosing spondylitis and rheumatoid arthritis. *PLoS One* 2012; **7**: e31000.
5. Lubberts E. The IL-23-IL-17 axis in inflammatory arthritis. *Nat Rev Rheumatol* 2015; **11**: 415–429.
6. Chen DY, Chen YM, Chen HH *et al*. Increasing levels of circulating Th17 cells and interleukin-17 in rheumatoid arthritis patients with an inadequate response to anti-TNF-α therapy. *Arthritis Res Ther* 2011; **13**: R126.
7. Robert M, Miossec P. IL-17 in rheumatoid arthritis and precision medicine: from synovitis expression to circulating bioactive levels. *Front Med* 2018; **5**: 364.
8. Rao DA, Gurish MF, Marshall JL *et al*. Pathologically expanded peripheral T helper cell subset drives B cells in rheumatoid arthritis. *Nature* 2017; **542**: 110–114.
9. Cho BA, Sim JH, Park JA *et al*. Characterization of effector memory CD8+ T cells in the synovial fluid of rheumatoid arthritis. *J Clin Immunol* 2012; **32**: 709–720.
10. Carvalheiro H, Duarte C, Silva-Cardoso S *et al*. CD8+ T cell profiles in patients with rheumatoid arthritis and their relationship to disease activity. *Arthritis Rheumatol* 2015; **67**: 363–371.
11. Cammarata I, Martire C, Citro A *et al*. Counter-regulation of regulatory T cells by autoreactive CD8+ T cells in rheumatoid arthritis. *J Autoimmun* 2019; **99**: 81–97.
12. Watanabe H, Gehad A, Yang C *et al*. Human skin is protected by four functionally and phenotypically discrete populations of resident and recirculating memory T cells. *Sci Transl Med* 2015; **7**: 279ra39.
13. Topham DJ, Reilly EC. Tissue-resident memory CD8+ T cells: from phenotype to function. *Front Immunol* 2018; **9**: 515.
14. Mackay LK, Rahimpour A, Ma JZ *et al*. The developmental pathway for CD103+CD8+ tissue-resident memory T cells of skin. *Nat Immunol* 2013; **14**: 1294–1301.
15. Djenidi F, Adam J, Goubar A *et al*. CD8+CD103+ tumor-infiltrating lymphocytes are tumor-specific tissue-resident memory T cells and a prognostic factor for survival in lung cancer patients. *J Immunol* 2015; **194**: 3475–3486.
16. Mueller SN, Mackay LK. Tissue-resident memory T cells: local specialists in immune defence. *Nat Rev Immunol* 2016; **16**: 79–89.
17. Mueller SN, Gebhardt T, Carbone FR, Heath WR. Memory T cell subsets, migration patterns, and tissue residence. *Annu Rev Immunol* 2013; **31**: 137–161.
18. Gebhardt T, Wakim LM, Eidsmo L *et al*. Memory T cells in nonlymphoid tissue that provide enhanced local immunity during infection with herpes simplex virus. *Nat Immunol* 2009; **10**: 524–530.
19. Duhen T, Duhen R, Montler R *et al*. Co-expression of CD39 and CD103 identifies tumor-reactive CD8 T cells in human solid tumors. *Nat Commun* 2018; **9**: 2724.
20. Cheuk S, Schlums H, Gallais Serezal I *et al*. CD49a expression defines tissue-resident CD8+ T cells poised for cytotoxic function in human skin. *Immunity* 2017; **46**: 287–300.
21. Petrelli A, van Wijk F. CD8+ T cells in human autoimmune arthritis: the unusual suspects. *Nat Rev Rheumatol* 2016; **12**: 421–428.
22. Bishu S, El Zaatari M, Hayashi A *et al*. CD4+ tissue-resident memory T-cells expand and are a major source of mucosal tumor necrosis factor α in active Crohn's disease. *J Crohns Colitis* 2019; **13**: 905–915.
23. Wu H, Liao W, Li Q *et al*. Pathogenic role of tissue-resident memory T cells in autoimmune diseases. *Autoimmun Rev* 2018; **17**: 906–911.
24. Petrelli A, Mijnheer G, van Konijnenburg DPH *et al*. PD-1+CD8+ T cells are clonally expanding effectors in human chronic inflammation. *J Clin Invest* 2018; **128**: 4669–4681.
25. Khandpur R, Carmona-Rivera C, Vivekanandan-Giri A *et al*. NETs are a source of citrullinated autoantigens and stimulate inflammatory responses in rheumatoid arthritis. *Sci Transl Med* 2013; **5**: 178ra140.
26. Konig MF, Andrade F. A critical reappraisal of neutrophil extracellular traps and NETosis mimics based on differential requirements for protein citrullination. *Front Immunol* 2016; **7**: 461.
27. Mackay LK, Wynne-Jones E, Freestone D *et al*. T-box transcription factors combine with the cytokines TGF-β and IL-15 to control tissue-resident memory T cell fate. *Immunity* 2015; **43**: 1101–1111.

28. Park MK, Her YM, Cho ML *et al*. IL-15 promotes osteoclastogenesis via the PLD pathway in rheumatoid arthritis. *Immunol Lett* 2011; **139**: 42–51.
29. Romero P, Fert-Bober J, Nigrovic PA *et al*. Immune-mediated pore-forming pathways induce cellular hypercitrullination and generate citrullinated autoantigens in rheumatoid arthritis. *Sci Transl Med* 2013; **5**: 1–12.
30. Boeltz S, Amini P, Anders HJ *et al*. To NET or not to NET:current opinions and state of the science regarding the formation of neutrophil extracellular traps. *Cell Death Differ* 2019; **26**: 395–408.
31. Kataoka T, Shinohara N, Takayama H *et al*. Concanamycin A, a powerful tool for characterization and estimation of contribution of perforin-and Fas-based lytic pathways in cell-mediated cytotoxicity. *J Immunol* 1996; **156**: 3678–3686.
32. Spreafico R, Rossetti M, van Loosdregt J *et al*. A circulating reservoir of pathogenic-like CD4$^+$ T cells shares a genetic and phenotypic signature with the inflamed synovial micro-environment. *Ann Rheum Dis* 2016; **75**: 459–465.
33. Ishigaki K, Shoda H, Kochi Y *et al*. Quantitative and qualitative characterization of expanded CD4$^+$ T cell clones in rheumatoid arthritis patients. *Sci Rep* 2015; **5**: 1–9.
34. Raychaudhuri S, Sandor C, Stahl EA *et al*. Five amino acids in three HLA proteins explain most of the association between MHC and seropositive rheumatoid arthritis. *Nat Genet* 2012; **44**: 291–296.
35. Adachi T, Kobayashi T, Sugihara E *et al*. Hair follicle-derived IL-7 and IL-15 mediate skin-resident memory T cell homeostasis and lymphoma. *Nat Med* 2015; **21**: 1272–1279.
36. Ariotti S, Hogenbirk MA, Dijikgraaf FE *et al*. Skin-resident memory CD8$^+$ T cells trigger a state of tissue-wide pathogen alert. *Science* 2014; **346**: 101–105.
37. Beura LK, Fares-Frederickson NJ, Steinert EM *et al*. CD4$^+$ resident memory T cells dominate immunosurveillance and orchestrate local recall responses. *J Exp Med* 2019; **216**: 1214–1229.
38. Richmond JM, Strassner JP, Zapata L *et al*. Antibody blockade of IL-15 signaling has the potential to durably reverse vitiligo. *Sci Trans Med* 2018; **10**: eaam7710.
39. Douda DN, Khan MA, Grasemann H, Palaniyar N. SK3 channel and mitochondrial ROS mediate NADPH oxidase-independent NETosis induced by calcium influx. *Proc Natl Acad Sci USA* 2015; **112**: 2817–2822.
40. Kuhns DB, Long Priel DA, Chu J, Zarember KA. Isolation and functional analysis of human neutrophils. *Curr Protoc Immunol* 2015; **111**: 7–23.

Supporting Information

Additional supporting information may be found online in the Supporting Information section at the end of the article.
Supplementary figures 1-8
Supplementary tables 1-3